SLAC–PUB–95–6457

Measurements of the Neutron Polarized Structure Function at SLAC*

CHARLES C. YOUNG
Stanford Linear Accelerator Center
Stanford University, Stanford, CA 94309
representing the E-142 Collaboration+

ABSTRACT

Detailed measurements of unpolarized or spin-averaged nucleon structure functions over the past two decades have led to detailed knowledge of the nucleon's internal momentum distribution. Polarized nucleon structure function measurements, which probe the nucleon's internal spin distribution, started at SLAC in 1976. E-142 has recently measured the neutron polarized structure function $g_1^n(x)$ over the range $0.03 < x < 0.6$ at an average Q^2 of 2 GeV^2 and found the integral $I^n = \int_0^1 g_1^n(x)dx = -0.022 \pm 0.011$. E-143, which took data recently, has measured g_1^p and g_1^d. Two more experiments (E-154 and E-155) will extend these measurements to lower x and higher Q^2.

* Work supported by Department of Energy contract DE–AC03–76SF00515.

+ P.L. Anthony, R.G. Arnold, H.R. Band, H. Borel, P.E. Bosted, V. Breton, G.D. Cates, T.E. Chupp, F.S. Dietrich, J. Dunne, R. Erbacher, J. Fellbaum, H. Fonvieille, R. Gearhart, R. Holmes, E.W. Hughes, J.R. Johnson, D. Kawall, C. Keppel, S.E. Kuhn, R.M. Lombard-Nelsen, J. Marroncle, T. Maruyama, W. Meyer, Z.-E. Meziani, H. Middleton, J. Morgenstern, N.R. Newbury, G.G. Petratos, R. Pitthan, R. Prepost, Y. Roblin, S.E. Rock, S.H. Rokni, G. Shapiro, T. Smith, P.A. Souder, M. Spengos, F. Staley, L.M. Stuart, Z.M. Szalata, Y. Terrien, A.K. Thompson, J.L. White, M. Woods, J. Xu, C.C. Young, G. Zapalac

Presented at the International Workshop on Deep Inelastic Scattering and Related Subjects, Eilat, Isreal, February 6–11, 1994

1. Theoretical Background

1.1 Polarized Structure Functions $g_1(x)$ and $g_2(x)$

The differential cross section for scattering a polarized electron from a polarized nucleon is characterized by the formula:

$$\frac{d^2\sigma^{\uparrow\downarrow}}{dQ^2 d\nu} - \frac{d^2\sigma^{\uparrow\uparrow}}{dQ^2 d\nu} = \frac{4\pi\alpha^2}{Q^2E^2}\left[M(E+E'\cos\theta)G_1(Q^2,\nu) - Q^2G_2(Q^2,\nu)\right]$$

where $\uparrow\downarrow(\uparrow\uparrow)$ indicates longitudinal target spin antiparallel (parallel) to the incident electron spin. The incident electron beam energy is E, E' is the scattered electron energy, and θ is the electron scattering angle. The mass of the nucleon is M, $\nu = (E - E')$ is the energy loss of the electron, $-Q^2$ is the square of the four momentum of the virtual photon, and α is the fine structure constant. In the scaling limit, the functions $G_1(Q^2,\nu)$ and $G_2(Q^2,\nu)$ can be written in terms of the polarized structure functions $g_1(x)$ and $g_2(x)$:

$$g_1(x) = M^2\nu G_1(Q^2,\nu),$$
$$g_2(x) = M\nu^2 G_2(Q^2,\nu),$$

where $x = Q^2/(2M\nu)$ is the scaling variable. It can be shown that g_1 is given by

$$g_1(x) = \frac{F_2(x,Q^2)}{2x(1+R)}\left[A_1(x,Q^2) + \gamma A_2(x,Q^2)\right],$$

where F_2 is the unpolarized structure function, A_1 is the cross-section asymmetry for fully polarized virtual photon on logitudinally polarized nucleons, α is a kinematic factor given by $\alpha^2 = (4M^2X^2)/Q^2$, A_2 is a similar cross section asymmetry for transversely polarized nucleon, and R is the ratio of longitudinally to transversely polarized photon cross-sections (σ_L/σ_T).Virtual photon asymmetries A_1 and A_2 are related to the corresponding cross section asymmetry for electrons $A_{\|}(x,Q^2)$ and $A_{\perp}(x,Q^2)$ by

$$A_{\|} = D(A_1 + \eta A_2),$$
$$A_{\perp} = d(A_2 - \zeta A_1),$$

where $\|(\perp)$ refers to target nucleon spin aligned along (transverse to) the electron beam spin direction. The kinematic factor relating electron polarization to that of the virtual photon is given by

$$D = \frac{1-\varepsilon\left(\frac{E'}{E}\right)}{1+\varepsilon R}$$

Note that $\varepsilon^{-1} = 1 + 2\left(1+\frac{\nu^2}{Q^2}\right)\tan^2\left(\frac{\theta}{2}\right)$ $\eta = \left(\varepsilon\sqrt{Q^2}\right)/(E - E'\varepsilon)$, $d = D\sqrt{(2\varepsilon)/(1+\varepsilon)}$, and $\zeta = \eta(1+\varepsilon)/\varepsilon$. Thus, measurements of $A_{\|}$ and $A_{\perp}$ give A_1 and A_2, and hence will allow a determination of g_1. The kinematic factors ensure that g_1 is insensitive to measurement errors on $A_{\perp}$. Since ζ is small, $A_{\perp}$ depends primarily on A_2, which is limited by unitarity considerations to $|A_2| \le \sqrt{R}$. Since R is known to be small, and γ can also be shown to be small for the kinematics of this experiment, the second term in g_1 is relatively unimportant. The behavior of g_1 near x=0 and x=1 is known. As $x \to 1$, g_1 must go to zero as $F_2 \to 0$ since the other factors are finite. Regge theory is reliable at low x and predicts that $g_1(x) \propto x^{\alpha}$ as $x \to 0$.

The equation for $g_1(x)$ can be easily understood within the quark parton model (QPM). It is interpreted as the difference distribution between quarks whose spin is parallel and anti-parallel to the nucleon's spin.

$$g_1(x) = \frac{1}{2}\sum e_i^2 (q_i^{\uparrow}(x) - q_i^{\downarrow}(x))$$

Similarly, the unpolarized structure function F_1 is interpreted as the sum.

$$F_1(x) = \frac{1}{2}\sum e_i^2 (q_i^{\uparrow}(x) + q_i^{\downarrow}(x))$$

The arrow $\uparrow(\downarrow)$ indicates quark spin parallel(antiparallel) to nucleon spin. It can be seen that the ratio of these two equations together with the well known relationship between F_1 and F_2 yields the leading term in g_1 above.

1.2 Sum Rules

While there are no rigorous predictions of the detailed functional forms of g_1^p(x) and g_1^n(x), Bjorken derived a fundamental sum rule on their integrals.[1] Denoting by I^p the integral $\int_0^1 g_1^p(x)dx$ for a proton and I^n the integral $\int_0^1 g_1^n(x)dx$ for a neutron, The Bjorken sum rule is given by:

$$I^p - I^n = \frac{1}{6}\left(\frac{g_A}{g_V}\right)\left[1 + O(\alpha_s(Q^2))\right],$$

where g_A and g_V are the axial and vector coupling constants measured very accurately in nucleon β decays. QCD corrections are given to first order by $-(\alpha_S/\pi)$.[2] Violations of the Bjorken sum rule would seriously undermine the validity of QCD.

Independent sum rules for I^p and I^n have been derived by Ellis and Jaffe:[3]

$$I^p = \frac{1}{18}(9F - D)\left[1 + O\left(\alpha_s\left(Q^2\right)\right)\right]$$

$$I^n = \frac{1}{18}(6F - 4D)\left[1 + O\left(\alpha_s\left(Q^2\right)\right)\right]$$

where F and D are coupling constants measured in hyperon decay.[4] The derivation relies upon SU(3) flavor symmetry and the assumption of an unpolarized strange sea. Thus, violations of the Ellis-Jaffe sum rules need not pose a fundamental problem for QCD.

---

[1] J.D. Bjorken, Phys. Rev. 148 (1966) 1467, Phys. Rev. D1 (1970) 1376.

[2] Higher order corrections have also been calculated. See S.A. Larin and J.A.M. Vermascren, Phys. Lett. B259 (1991) 345.

[3] J. Ellis and R.L. Jaffe, Phys. Rev D9 (1974) 1444. See S.A. Larin, Phys. Lett. B334 (1994) 192, and A. L. Kataev, Report No. CERN-TH- 7427/94 for QCD corrections.

1.3 Quark Spin Contribution

The total quark contribution to nucleon spin, Δq, is the sum of the individual quark flavor contributions Δu, Δd, and Δs.

$$\Delta u = \int_0^1 \left[u^{\uparrow}(x) - u^{\downarrow}(x) \right] dx,$$

where $\uparrow(\downarrow)$ indicates quark spin parallel (antiparallel) to nucleon spin. In QPM, these quantities are related to experimental measurements of hyperon decay constants, beta decay measurements,[5] and polarized structure functions:

$$D - F = \Delta s - \Delta d \approx 0.339 \pm 0.001,$$

$$\frac{g_A}{g_V} = \Delta u - \Delta d \approx 1.257 \pm 0.003,$$

$$I^p = \frac{1}{2}\left[\frac{4}{9}\Delta u + \frac{1}{9}\Delta d + \frac{1}{9}\Delta s \right],$$

$$I^n = \frac{1}{2}\left[\frac{1}{9}\Delta u + \frac{4}{9}\Delta d + \frac{1}{9}\Delta s \right].$$

By combining the first two equations with a measurement of either I^p or I^n, the individual quark spin contributions can be calculated.

SLAC Experiments E-80[6] and E-130[7] made the first measurements of polarized proton structure function. They were followed by the European Muon Collaboration group (EMC). The latter's measurement[8] of $I^p = 0.126 \pm 0.018$ implies

$$\Delta u = 0.74 \pm 0.05,$$

$$\Delta d = -0.52 \pm 0.05,$$

$$\Delta s = -0.18 \pm 0.06,$$

$$\Delta q = \Delta u + \Delta d + \Delta s = 0.05 \pm 0.16.$$

This rather surprising conclusion that quarks carry little of the spin of the proton has been dubbed the Spin Crisis. The results also imply that there is substantial strange sea polarization. There has been much theoretical speculation on this.[9]

---

[4] R.L. Jaffe and A.V. Manohar, Nucl. Phys. B337 (1990) 509, F.E. Close and R.G. Roberts, Phys. Lett. B316 (1993) 165.

[5] Review of Particle Properties, Phys. Rev. D45 (1992) 1.

[6] M.J. Alguard et al, Phys. Rev. Lett. 37 (1976) 1258 and M.J. Alguard et al, Phys. Rev. Lett. 37 (1976) 1261.

[7] G. Baum et al, Phys. Rev. Lett. 51 (1083) 1135.

[8] J. Ashman et al, Phys. Lett. B206 (1988) 364 and J. Ashman et al, Nucl. Phys. B328 (1989) 1.

[9] G. Altarelli et al, Phys. Lett. B212 (1988) 391, R.D. Carlitz et al, Phys. Lett. B214 (1988) 229, S. Brodsky et al, Phys. Lett. B206 (1988) 309, J. Ellis et al, Phys. Lett. B213 (1988) 73.

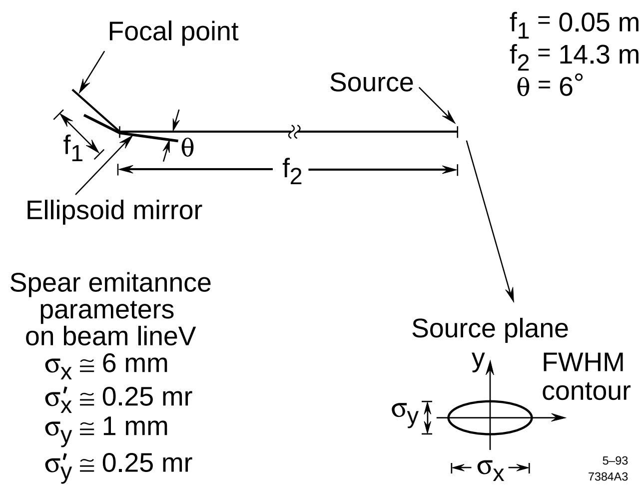

Figure 1: Schematic of the SLAC polarized electron source.

2. SLAC Experiment E-142

The goal of SLAC experiment E-142[10] is to perform a high statistics measurement of the neutron's polarized structure function g_1^n and hence obtain I^n. This can be combined with a measurement of I^p to check the Bjorken sum rule. It can also be used independently of I^p to calculate quark contribution to nucleon spin.

2.1 Beam

Circularly polarized light impinges on an AlGaAs cathode[11] as shown in Fig. 1. Conservation of angular momentum restricts ionization from certain energy-degenerate spin states, and their relative populations give rise to a net electron beam polarization P_b of typically 39% in this experiment. See Table I for typical beam parameters. Beam polarization was measured with Møller scattering. Polarization was stable over the entire run. Polarization sign was chosen randomly on a pulse by pulse basis; thus, false asymmetries due to changes in detector acceptance or response are minimized

Table I: Beam parameters for E-142.

Energy, E	19, 22, and 26 GeV
Intensity	$0.5-2\times10^{11}$ electrons per pulse
Pulse duration	0.8 – 1.4 msec
Polarization, P_b	$38.8\pm1.6\%$
Polarization Reversal	random, pulse by pulse
Repetition Rate	120 Hz

[10] P.L. Anthony et al, Phys. Rev. Lett. 71 (1993) 959.
[11] T. Maruyama et al, J. Appl. Phys. 73 (1993) 5189.

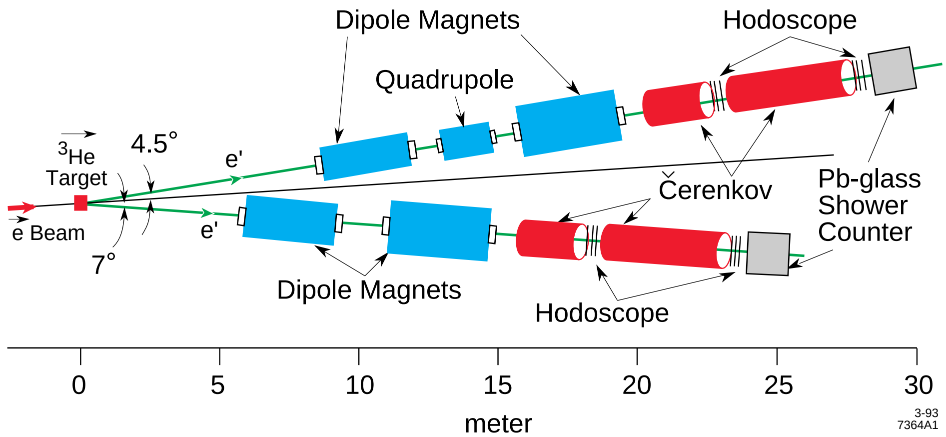

Figure 2: Schematic layout of the polarized ^{3}He target. Five sets of lasers optically pump rubidium vapor in the top chamber, and ^{3}He nuclei acquire polarization through spin exchange collisions. Incident electrons scatter off nuclei in the bottom chamber. Two sets of Helmholtz coils hold the target spin in either longitudinal or transverse directionss. Drive and pickup coils are used to measured polariztion.

2.2 Target

The target uses ^{3}He, which is polarized through spin exchange collisions with optically pumped polarized rubidium vapor.[12] A two-chamber design was used.[13] Figure 2 shows the upper pumping chamber pumped by five high powered laser systems producing up to 20 W of infrared laser light. The lower target chamber has a length of 30 cm with 0.012-cm-thick glass end windows. It was filled with 2.3 x 10^{20} ^{3}He atoms/cc. The ^{3}He target polarization P_t was measured using nuclear magnetic resonance (NMR) techniques. A precision of $\Delta P_t/P_t$ = 7% was achieved, P_t varying slowly between 30% and 40% during the experiment, and its direction reversed frequently. Data were taken with target polarization along and transverse to beam direction to measure both $A_{||}$ and $A_{\perp}$.

The exclusion principle ensures that the two proton spins are antiparallel in the ground state ^{3}He wave function. Protons do not contribute to measured asymmetry.[14] This contrasts with a deuteron target for which the proton's relatively large asymmetry must be subtracted statistically.

---

[12] T.E. Chupp et all, Phys. Rev. C45 (1992) 915.

[13] T.E. Chupp et al, Phys. Rev. C36 (1987) 2244.

[14] Higher order corrections are ~10±2%. See for example R.M. Woloshin, Nucl. Phys. 496A (1989) 749, and Ciofi degli Atti et al, Univ. of Perugia Preprint 75/93. Given the small measured asymmetries, a 1-σ change in results requires a 30% theoretical change.

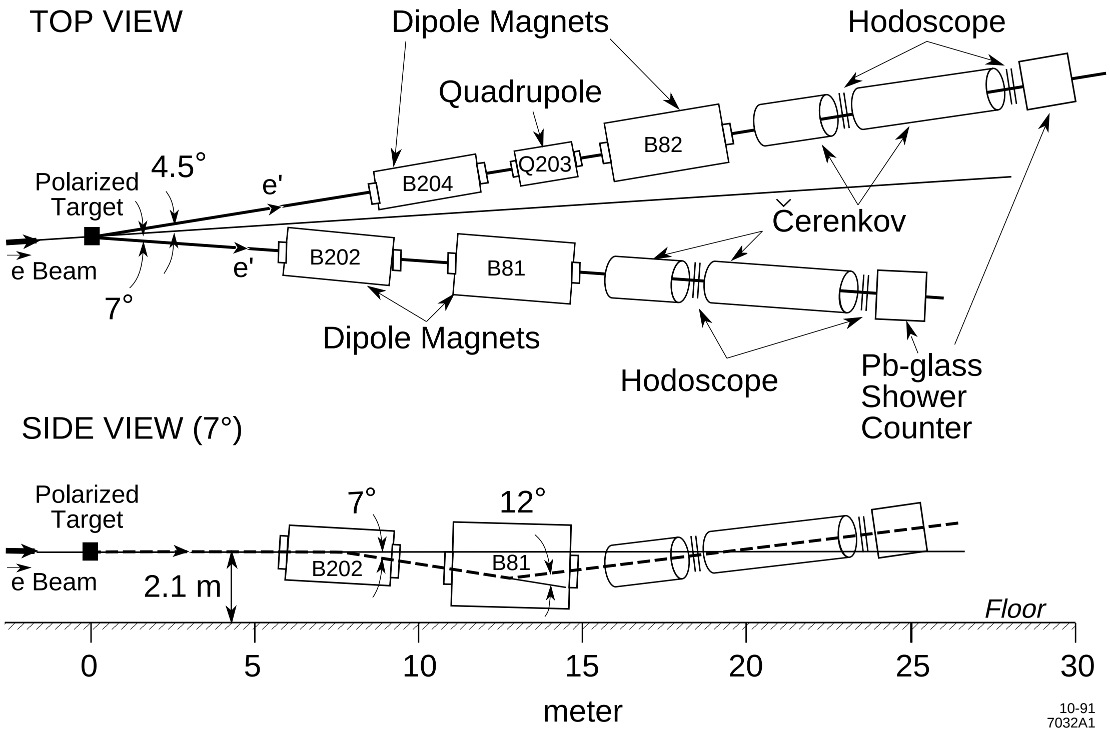

Figure 3: Experimental layout consisting of two independent spectrometers.

2.3 Spectrometer

Scattered electrons are detected in two independently operating spectrometers.[15] The scattering angles are 4.5^o and 7^o, respectively, measuring overlapping ranges of x from 0.03 to 0.6 with Q^2 greater than ≈ 1 GeV^2. Approximately 4 x 10^8 events were collected. Magnetic deflection and scintillation hodoscopes measure momentum with a precision of ~3%. The 200-element 24-radiation-length lead glass array measures electron energy with a precision of $\sigma_{E'}/E' \approx 15\%/\sqrt{E'(GeV)}$. Figure 4 shows these resolutions as functions of E'. Nitrogen filled threshold Cerenkov counters operating with ~6 photoelectrons each provide efficient electron identification. Electrons are further identified by the pattern of energy deposition[16] and a comparison of energy with momentum.

2.4 Analysis

The experimental asymmetry $A_{||}$ is derived from the measured counting rate asymmetry Δ:

$$\Delta = \frac{\left(N^{\uparrow\downarrow} - N^{\uparrow\uparrow}\right)}{\left(N^{\uparrow\downarrow} + N^{\uparrow\uparrow}\right)} = A_{||} P_b P_t f,$$

where $N^{\uparrow\downarrow}(N^{\uparrow\uparrow})$ represents the number of scattered electrons in the spectrometer per incident beam electron when the beam and target spins are antiparallel(parallel). The dilution factor f is the fraction of events originating from polarized neutrons in the target.

---

[15] G.G. Petratos et al, SLAC–PUB–5678 (1991)

[16] C. Guichency, These de Docteur en Sciences, Univ. of Clermont-Ferrand (1992)

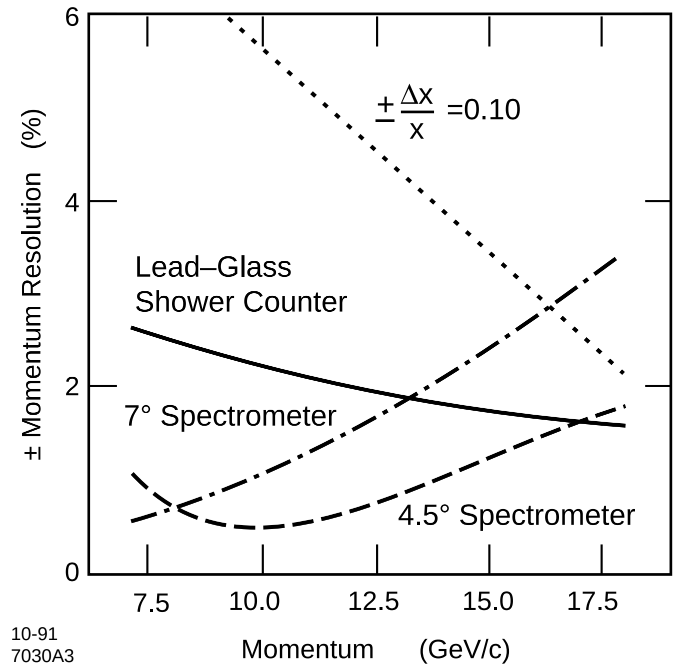

Figure 4: Momentum and energy resolution of the E-142 spectrometer.

All counting rates are corrected for dead time and normalized to the same incident charge for the two beam polarizations. Beam charge differences between the two beam polarization directions was measured to be less than one part in 10^4.

Electron background from charge symmetric processes was determined to be ~5% of the electron sample at low x. It decreases with increasing x. This was determined by reversing the polarity of the spectrometer magnets to measure positrons. Background from pions was studied by comparing track momentum with shower counter energy. Pions constitute ~2% of the electron sample at low x. Contaminations at high x were negligible.

The dilution factor f was measured empirically by filling the target cell to different pressures, allowing a statistical separation of events coming from ^{3}He and from the glass. The dilution factor $f = 0.11 \pm 0.02$ is a slow function of x. This 15% uncertainty is the largest single contribution to the systematic uncertainty on A_1^n.

False asymmetries have been studied by comparing data sets not expected to have any asymmetry, e.g., target spins in opposite directions. All false asymmetries are consistent with zero.

Internal[17] and external[18] radiative corrections gave rise to a relative change in the asymmetry from $30 \pm 15\%$ at low x to $5 \pm 2\%$ at high x. These uncertainties include variations due to model dependence of the corrections.

Small corrections due to the polarization of the protons in ^{3}He (~–2.7% per proton) were applied[19,20] to obtain neutron asymmetry from ^{3}He asymmetry.

---

[17] The formulae from Kuhto and Shimeiko were integrated without peaking approximations. T.V. Kuhkto and N.M. Shimeiko, Nucl. Phys. B219 (1983) 412.

[18] The corrections are small because of the thin (~3% radiation length) gas target. L.W. Mo and Y.S. Tsai, Rev. Mod. Phys. 41 (1969) 205.

2.5 Results

Figure 5 shows A_1^n as a function of Q^2 for different x ranges. Results are consistent with being Q^2-independent over the measured range.[21] Data over all Q^2 will therefore be averaged when studying x dependence. Measured neutron asymmetries and structure functions are given in Table II. Figure 6 shows A_1^n and g_1^n with statistical and systematic uncertainties added in quadrature as functions of x. They are the most precise measurements at this time.[22]

The integral of $g_1^n(x)$ over the measured x range is therefore –0.019 ± 0.007 (stat) ± 0.006 (sys) at an average Q^2 of 2 GeV^2. Measurements of $g_1^n(x)$ at different values of x have different average Q^2. Using the measured Q^2 dependence of unpolarized structure functions, they can be corrected to a common Q^2 value of 2 GeV^2 before integration over x. The integral result remains unchanged. Systematic uncertainties on I^n are summarized in Table 3.

Table II: Neutron asymmetry results and structure functions from E-142. The first error is statistical and the second systematic.

<x>	$\langle Q^2 \rangle$	A_1^n	ΔA_1^n	g_1^n	Δg_1^n
0.025	0.96	0.066	.109/.019	0.267	.446/.100
0.035	1.1	-0.058	.056/.021	–0.175	.169/.052
0.050	1.3	-0.095	.033/.030	–0.228	.079/.061
0.078	1.6	-0.062	.031/.031	–0.095	.048/.026
0.124	2.3	-0.136	.030/.038	–0.133	.029/.031
0.175	2.7	-0.087	.041/.037	–0.057	.027/.014
0.248	3.1	-0.020	.046/.055	–0.008	.019/.006
0.344	3.4	0.029	.091/.068	0.006	.020/.003
0.466	5.2	0.030	.219/.100	0.003	.024/.002

---

[19] B. Blankleider and R.M. Woloshyn, Phys. Rev. C29 (1984) 538.

[20] J.L. Friar et al, Phys. Rev. C42 (1990) 2310.

[21] The SMC collaboration has combined their deuteron results with proton results from SLAC E-80, E-130, and the EMC collaboration at Cern to derive A_1 for the neutron. These results extend to Q^2~25 GeV^2, and to within their much larger uncertainties do not observe any Q^2 dependence compared with the data reported here. See B. Adeva et al, Cern Preprint CERN–PPE/93–206.

[22] Neutron asymmetry results have also been measured by the SMC collaboration at Cern. See B. Adeva et al, Phys. Lett. B302 (1993) 533. The higher energy muon beam at Cern extends the measurement range to lower x; the lowest <x> = 0.009. Measurement precision is limited by statistics and false asymmetries due to acceptance variations.

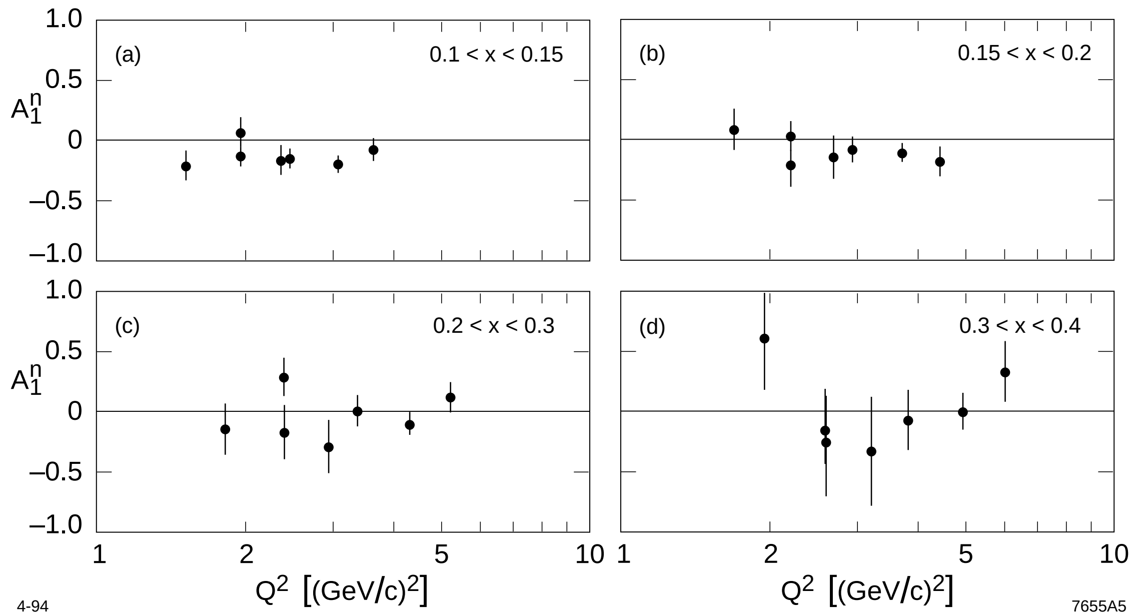

Figure 5: A_1^n vs Q^2 for four ranges of x. Results are independent of Q^2. Supply topdraw files.

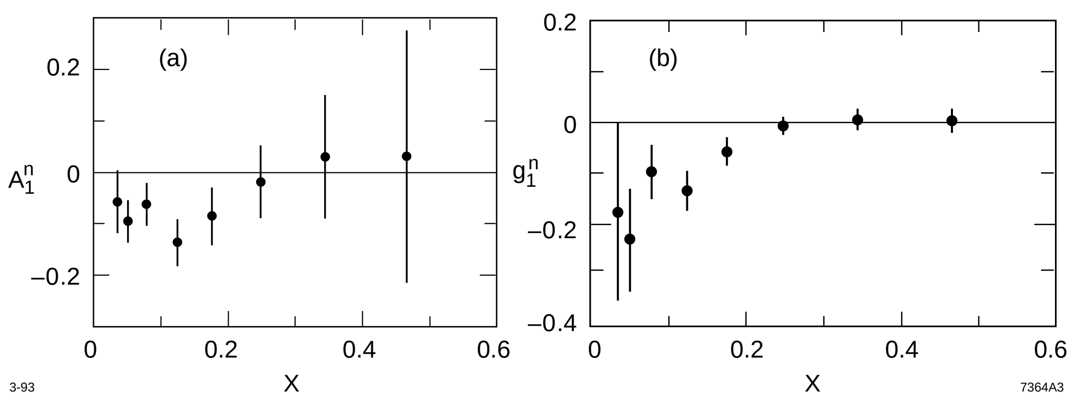

Figure 6: Results for neutron asymmetries A_1^n and the neutron spin structure function $g_1{}^n$ as functions of x averaged over Q^2. Statistical and systematic errors are added in quadrature.

Table III: Summary of systematic uncertainties and their effects on I^n.

Dilution Factor, f	0.003
A_2	0.003
F_2	0.002
Target polarization, P_t	0.002
Beam polarization, P_b	0.001
Radiative correction	0.001
R	0.001
Total	0.006

High x extrapolation contributes 0.003. Low x extrapolation is guided by Regge form $A_1^n(x) \sim x^{\alpha}$, and contributes –0.006. Systematic uncertainties from extrapolation have been estimated by varying the range of the fit and are taken to be equal to the magnitude of the contributions. Spin Muon Collaboration (SMC) measurements at lower x are compatible with the E-142 extrapolation.[23] Thus, the integral of g_1^n over the range x = 0 to x=1 has been determined to be –0.022 ± 0.007 ± 0.009, where the first error is statistical and the second systematic. Adding the two uncertainties in quadrature yields I^n = –0.022 ± 0.011.

Table IV: Determination of the integral of $g_1^n(x)$ by E-142.

	Integral	Statistical	Systematic
Measured x range	–0.019	0.007	0.006
Low x extrapolation	–0.006		0.006
High x extrapolation	0.003		0.003
I^n	–0.022	0.007	0.009

2.6 Quark Spin and Sum Rule

Using this value of I^n in place of the EMC measurement of I^p, one finds that

$$\Delta u = 0.93 \pm 0.03,$$
$$\Delta d = -0.33 \pm 0.03,$$
$$\Delta s = 0.01 \pm 0.03,$$
$$\Delta q = \Delta u + \Delta d + \Delta s = 0.60 \pm 0.10.$$

In contrast to the conclusions based on I^p, quarks are found to carry approximately half the spin of the nucleon, and strange sea polarization is small.

The most precise test of the Bjorken sum rule is obtained by combining this [ref] determination of I^n with the preliminary results of E143 on the proton I^p = 0.129 ± 0.004 (stat.) ± 0.009 (sys.), to give the experimental result $I^p - I^n$ = 0.151 ± 0.015. This is an agreement at the 1-σ level with the sum rule prediction of 0.164 ± 0.008, where we have used α_S = 0.39 ± 0.007 at Q^2 = 2 GeV^2 to evaluate QCD corrections. Higher twist effects have not been included in the theoretical prediction.

3. Other Polarized Structure Function Experiments at SLAC

3.1 Experiment E-143

Experiment E-143 measures the polarized structure functions of the proton and deuteron with polarized NH_3 and ND_3 targets, respectively. Neutron results will be obtained by subtraction. Data were taken from November 1993 through February 1994. Beam parameters are similar to those for E-142, but with higher beam energy (29 GeV) and

[23] See Fig. 3 in B. Adeva et al, Cern Preprint CERN–PPE/93–206.

polarization. The use of a strained GaAs cathode[24] has led to beam polarization of ~85%. The expected precision on A_1 of the proton and deuteron are compared in Fig. 7 with that of existing data.

3.2 50-GeV Program

An upgrade of the beam line from 30 GeV to 50 GeV is in progress, and two experiments have been approved to continue precision measurements of polarized nucleon structure functions. Beam polarizations of ~85% are expected. E-154 will use an improved ^{3}He target, and E-155 will use NH_3 and ND_3 targets. Spectrometers will be rebuilt at 2.75^o and 5.5^o to accommodate the new kinematics. Typical Q^2 will increase from ~ 2 GeV^2 (E-142) to ~ 5 GeV^2, with substantial data above 10 GeV^2. The lowest x (with Q^2 > 1 GeV^2) is reduced fom ~0.035 to ~0.018. Figure 8 shows the expected improvement to A_1^n. A summary of current and expected uncertainties on the integrals of structure functions is given in Table V. It is expected that the most stringent test of the Bjorken sum rule will use I^n from E-154 and I^p from E-155. This expected improvement is illustrated in Figs. 9 and 10.

---

[24] T. Maruyama et al, SLAC–PUB–5731, SLAC–PUB–6033, E. Garwin et al, SLAC–PUB–5751.

Table V: Measurement precision on I^p, I^n, and I^d. The three values are statistical, systematic and extrapolation uncertainties, respectively. E-130 and E-142 results have been published. E-143, E-154, and E-155 numbers are from their proposals.

	ΔI^p	ΔI^n	ΔI^d
E-130	.05 (combined)		
E-142		.007/.006/.007	
E-143	.003/.010/.002	.006/.012/.004	.005/.011/.004
E-154		.003/.003/.003	
E-155	.001/.008/.001	.002/.006/.002	.002/.008/.002

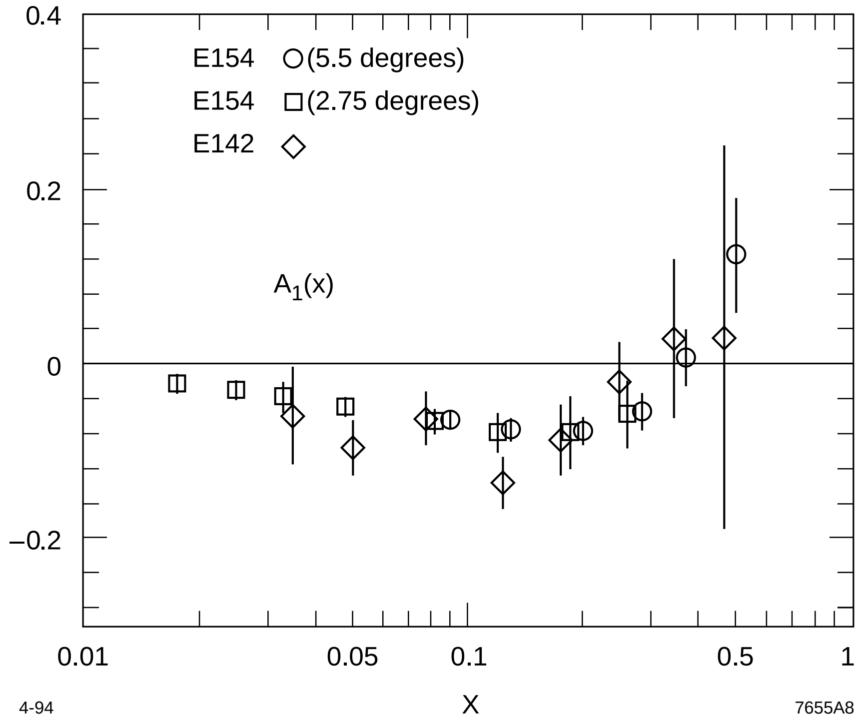

Figure 8: Expected measurement precision from E-154 compared with existing results.

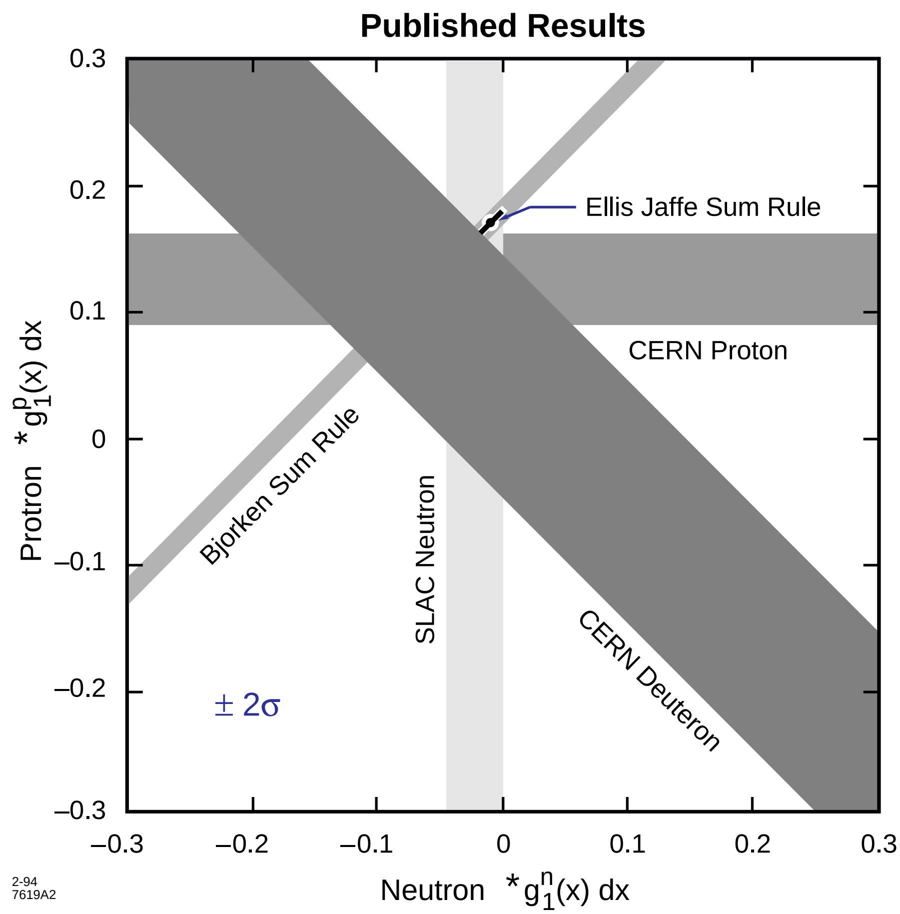

Figure 9: Precision of published results on the integrals of proton and neutron structure functions.

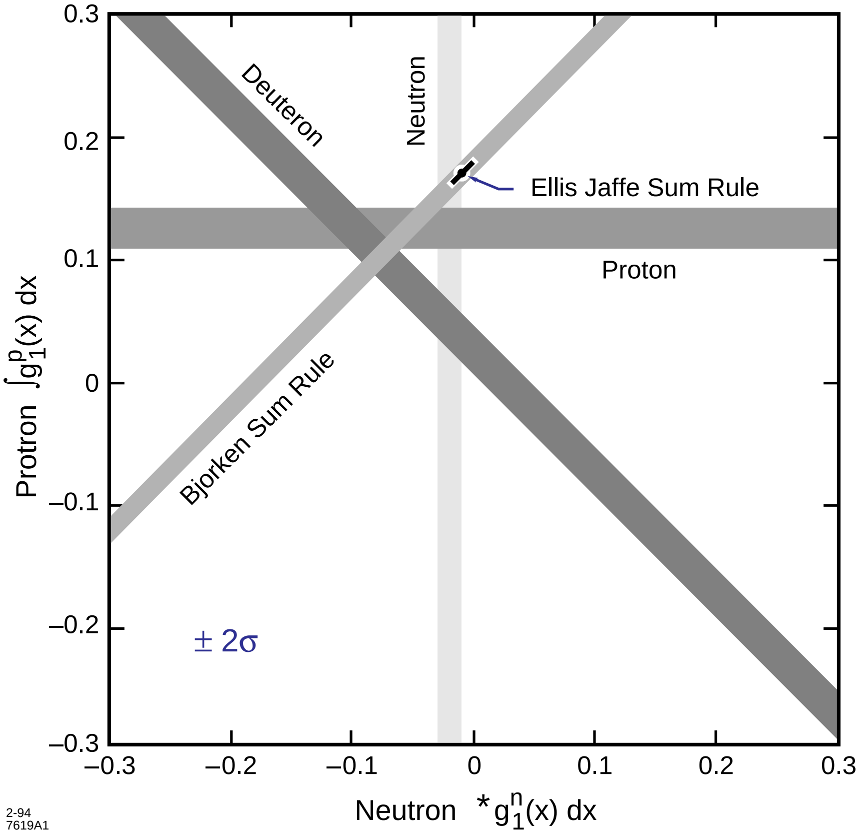

Figure 10: Expected precisions from experiments E-154 and E-155.